

Improved Chromaticity and Thermal Stability in White Light Emitting Diode Phosphor BaMgAl₁₀O₁₇: Eu²⁺, Mn²⁺

FENGCHAO WANG¹, ZHI ZHOU¹, SUQIN LIU^{1,*}, SHAOBO ZENG² and KUIMING JIANG²

¹Key Laboratory of Resources Chemistry of Nonferrous Metals, Ministry of Education, College of Chemistry and Chemical Engineering, Central South University, Changsha 410083, P.R. China

²Hunan Steady New Material Company, Shaoyang 422000, P.R. China

*Corresponding author: Tel/fax: +86 731 8879850; E-mail: sqliu2003@126.com

(Received: 8 December 2011;

Accepted: 16 June 2012)

AJC-11634

A highly efficient white light emitting diodes phosphor BaMgAl₁₀O₁₇: Eu²⁺, Mn²⁺ coating with MgF₂ layer was prepared and characterized. The phosphor consisted of a host material BaMgAl₁₀O₁₇ doped with 0.05 mol % Eu²⁺ and co-doped 0.05 mol % Mn²⁺. The mechanism of energy transfer between Eu²⁺ and Mn²⁺ is dipole-quadrupole. The phosphor coated with MgF₂ reveals that the durability is greatly enhanced 9.8 % comparison with uncoated phosphor after thermal degradation tests. The CIE chromaticity coordinates (0.335, 0.330) of the phosphor fabricated light-emitting diodes has a very close to that of the standard white light point of (0.333, 0.333). And the colour rendering index increases from 79 to 85 after the BaMgAl₁₀O₁₇: Eu²⁺ phosphor co-doped with Mn²⁺. All the result could conclude that co-doped and surface coated were two promises approaches for improving the colour rendering index of the near UV light-emitting diode and the stability of BaMgAl₁₀O₁₇: Eu²⁺, Mn²⁺ phosphor.

Key Words: White light-emitting diode, BaMgAl₁₀O₁₇: Eu²⁺ phosphor, Co-doped, Surface coated.

INTRODUCTION

Recently, great attention has been focused on phosphor converted white light-emitting diodes (LEDs), due to their excellent properties of high efficiency, long lifetime, low power consumption and environment-friendly characteristic compared with those of conventional incandescent and fluorescent lamps¹⁻⁵. Generally, a simple method to obtain white light is to combine a blue-emitting LED chip with a yellow-emitting phosphor. The first commercialized white LED was featured a blue LED in combination with Y₃Al₅O₁₂: Ce³⁺ (YAG: Ce³⁺) yellow phosphor⁶. However, the white light generated by combining a blue-light-emitting diode chip and a yellow phosphor exhibits low colour rendering index (CRI) and no full range of visible light⁷. A novel suggested solution is to use a UV chip with a primary emission of 370-410 nm instead of blue light-emitting diode⁸⁻¹⁰. That is, the UV LED chip is used as excitation light and combined with red/green/blue tricolour phosphors. To successfully generate the white light from LED, red, green and blue-emitting phosphors should work with high emission efficiency. In the current tricolour phosphors of the UV InGaN-LED chips, Y₂O₃S: Eu³⁺ for red, ZnS for green and BaMgAl₁₀O₁₇: Eu²⁺ for blue are generally used. Blue-emitting phosphor BaMgAl₁₀O₁₇: Eu²⁺ has the

problem of instability when used in the high powder LED, due to high temperature as high as 300 °C accompany with high powder LED¹¹.

Furthermore, the colour rendering index (CRI) is a very important parameter for LEDs. High colour rendering index is crucial for light, especial for interior illumination. Since improve the colour rendering index of fabricated LED was an interesting question for researcher.

To overcome the instability of the BaMgAl₁₀O₁₇: Eu²⁺ blue emitting phosphor, surface coating has attracted extensive attention when it used in the plasma display panels¹²⁻¹⁵. Magnesium fluoride is one of the most interesting metal fluorides due to the properties of low chemical reactivity even at elevated temperatures, low refractive index (1.38), high thermal stability, high corrosion resistance and significant hardness¹⁶⁻¹⁹. Therefore, MgF₂ has been extensively used as an antireflective and protective coating on glass optics because of its low refractive index. Magnesium fluoride can also be used as a promising UV transparent material due to the large band gap of MgF₂ (12.8 eV)²⁰⁻²⁴. Those entire make MgF₂ become an ideal coating material.

Meanwhile, by using the principle of energy transfer (ET) from sensitizer Eu²⁺ ions to activator Mn²⁺ ions, improve the colour rendering index of the phosphor has been investigated

in silicate^{25,26} and phosphate host^{27,28}. One of the purposes of this study is to apply the principle of energy transfer in the blue emitting phosphor BaMgAl₁₀O₁₇: Eu²⁺, which has not been reported in the literature.

In this paper, Mn²⁺ co-doped BaMgAl₁₀O₁₇: Eu²⁺ phosphors were synthesized by the solid-state reaction method. Surface coating with MgF₂ was used to the as-obtained phosphors. The phosphor converted white light emitting diode was successfully fabricated and the colour coordinates were measured as well as the colour rendering index. It was believed that co-doping and surface coating were the promising approaches for improve the colour rendering index of the white light emitting diode and the stability of BaMgAl₁₀O₁₇: Mn²⁺, Eu²⁺ phosphor, respectively.

EXPERIMENTAL

Synthesis: The raw materials used in the synthesis of the phosphor were as follows: BaCO₃, MgO, Al₂O₃, Mn₂O₃ and Eu₂O₃. All chemicals used in the experiments were of analytical purity, purchased from Sigma-Aldrich without further purification. The concentrations of BaCO₃, MgO and Al₂O₃ were fixed at 1 mol, 1 mol and 5 mol, respectively. The concentrations of Eu₂O₃ and Mn₂O₃ were fixed at 0.045 mol for both, which followed as reference²⁹.

After the ingredients were mixed thoroughly using ethanol, the mixture was pestled for 1 h in a crucible with a lid. The crucible was preheated at 300 °C for 1 h, cooled down and then sintered at 1300 °C for 2 h in H₂/N₂ reducing atmosphere. After these procedures, the BAM phosphor was blue white in body colour.

Surface coating: A series of concentration Mg(NO₃)₂ solutions were prepared. The NH₄F solution with certain concentration was added into it. A transparent colloidal product was obtained after a fully stirring and mixing. After static precipitation of the transparent colloidal product for several hours, the upper layer was discarded. The almost pure MgF₂ sol would be obtained by rinsing with distilled water for several times and then the sol could be served as the coating materials. Several sol samples were baked for 0.5 h at different temperatures. The as-prepared phosphors were mixed with dispersant and distilled water. Then a fixed quantify of MgF₂ sol was injected, adjusting pH value around 5, ball milling was employed to disperse the mixture. The phosphors evenly coated with MgF₂ could be fabricated by filtration, drying and baking for 0.5 h at 300 °C. The surface coated phosphors were obtained. In order to compare the thermal stability of the MgF₂ coated and uncoated sample, thermal degradation test have been carried out as follow, both of these two samples were calcined at 300 °C for 0.5 h in air atmosphere, their luminous properties were measured before and after the thermal degradation test.

After these procedures, the BAM phosphor was blue white in body colour. The phase purity of the sample was checked by Rigaku-D/max X-ray diffractometer (XRD) with condition of CuK_α, λ = 0.15148 nm, 40 kV, 200 mA. The morphology of material was examined by Nova Nano 230 scanning electron microscope (SEM) and JEOL-1230 transmission electron microscope. The measurements of photoluminescence and photoluminescence excitation spectra were performed using

a Hitachi F-4500 fluorescent spectrometer equipped with a xenon lamp at room temperature.

The white LEDs were fabricated by combining GaN-based UV LEDs (380 nm) and tricolour phosphors. The optical properties were evaluated by an Everfine PMS-80 UV-VIS-IR system under a current of 20 mA at room temperature.

RESULTS AND DISCUSSION

Crystallization analysis: Fig. 1 shows the XRD pattern of the samples, (a) is the Eu²⁺ doped phosphor by the solid-state reaction, (b) is the Mn²⁺ and Eu²⁺ co-doped phosphor and (c) is the co-doped samples coated with MgF₂. It showed that all XRD patterns are similar and in excellent agreement with the pattern of barium magnesium aluminate registered in the joint committee on powder diffraction strands card (JCPDS 084-0818). All the diffraction lines are assigned well to barium magnesium aluminate crystalline phase with the β-alumina structure corresponding to the space group P63/mmc and no extraneous diffraction peaks are found in the spectra, indicating that the phosphors obtained are monophasic barium magnesium aluminate and co-doping with Mn²⁺ and Eu²⁺ has no obvious influence on the structure of the host. The diffraction peaks of the samples after coating treatment do not change obviously comparing to that of untreated samples, which can be explained by the fact that MgF₂ sol has formed an amorphous film on the surface of BAM phosphors, similar to previous results in reference³⁰.

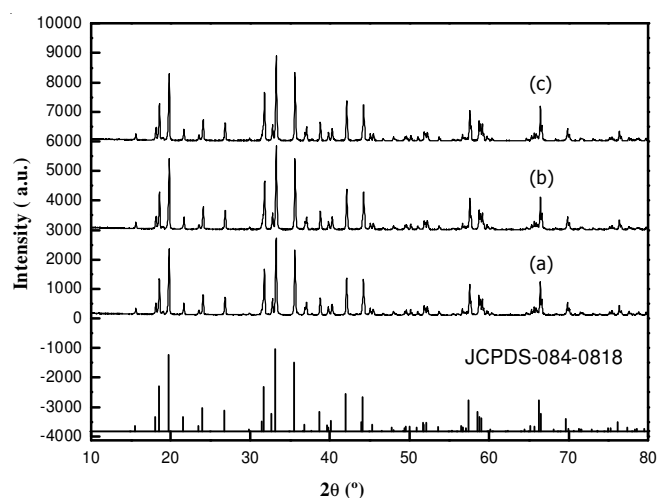


Fig. 1. XRD patterns of phosphor samples (a) BaMgAl₁₀O₁₇: Eu²⁺; (b) Mn²⁺ co-doped BaMgAl₁₀O₁₇: Eu²⁺; and (c) MgF₂ coated BaMgAl₁₀O₁₇: Eu²⁺, Mn²⁺

Morphology and composition analysis: Fig. 2 displays the SEM and TEM images of the coated and uncoated samples. A smooth and clean surface of the as-prepared BaMgAl₁₀O₁₇: Eu²⁺, Mn²⁺ powder is observed, as shown in Fig. 2(a) and Fig. 2(b). However, after coating with various amounts of MgF₂ gel, the surface of the MgF₂ coated phosphors show a coarse morphology, which is attributed to the formation of randomly distributed MgF₂ particles on the surface, as shown in Fig. 2(c). Fig. 2(d) is part amplification of Fig. 2(c), which shows a 25 nm to 30 nm thickness layer covering the phosphor. The coating layer on the surface of phosphor has to be transparent

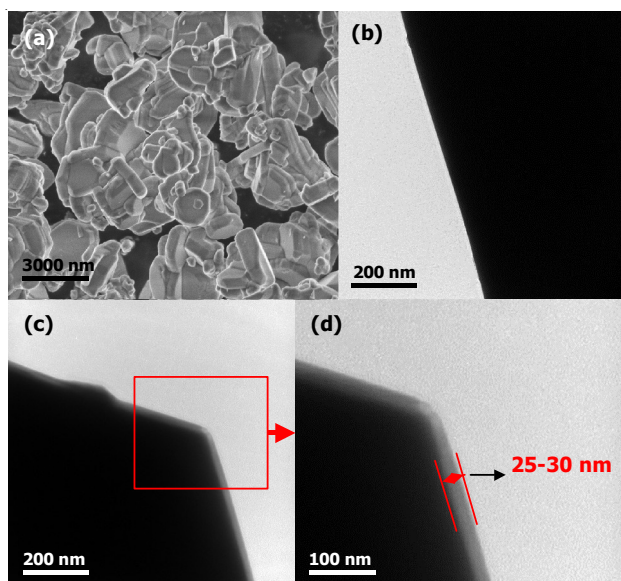


Fig. 2. SEM and TEM images of the samples (a) SEM image of as-prepared $\text{BaMgAl}_{10}\text{O}_{17}:\text{Eu}^{2+}, \text{Mn}^{2+}$; (b) TEM image of uncoated sample; (c) TEM image of MgF_2 coated sample; (d) higher magnification TEM image of the coated samples

and a precise amount of coating must cover the surface of the samples homogeneously to minimize the decrease the luminescence intensity. For the purpose of the increase stability of phosphor, a thick layer-like homogeneous coating would be also preferred³¹. Nano-coating layer with 25 nm to 30 nm thickness in this study support the phosphor to meet two requirement of transparent and protect the Eu^{2+} oxidized from thermal environment. The results above indicate that coating process is successful in this study.

The chemical composition of the coating layer was also confirmed with XPS. Fig. 3 shows the XPS result of the phosphor coated with MgF_2 nano-coating layer. The binding energy peak at 1305.08 eV ascribes to the $\text{Mg}1s$ and the peak at 685.08 eV corresponded to $\text{F}1s$. This fact implies that MgF_2 is coated on the surface of $\text{BaMgAl}_{10}\text{O}_{17}:\text{Eu}^{2+}, \text{Mn}^{2+}$ phosphor. The properties of high thermal stability, significant hardness and large band gap make MgF_2 become one of the best coating materials for phosphor.

Luminescent properties and energy transfer mechanism:

Fig. 4 shows the excitation and emission spectra of $\text{BaMgAl}_{10}\text{O}_{17}:\text{Eu}^{2+}, \text{Mn}^{2+}$. As shown in this figure, the samples has a broad excitation band from near UV to blue (from 250 to 450 nm) peaking at 355 nm. The absorption spectrum of Eu^{2+} is attributed to transitions from $4f^7$ ground state to the highest excited state ($5d$). BAM has the same structure as β -alumina³², which is built up of spinel blocks containing aluminum ions, magnesium ions and oxygen ions, separated by an intermediate layer containing barium ions and oxygen ions. Eu^{2+} ions are incorporated at barium sites with in the intermediate layers in $\text{BaMgAl}_{10}\text{O}_{17}:\text{Eu}^{2+}, \text{Mn}^{2+}$. Due to the $4f^65d^1-4f^7$ transition of the Eu^{2+} ion, the samples have a strong emission band peak at 455 nm with a full-width half-maximum (FWHM) of 90 nm. After co-doping Mn^{2+} with Eu^{2+} , the samples show a second intense peak in the emission spectra, which centered at 524 nm with a FWHM of 40 nm. This is attributed to the spin forbidden ${}^4\text{T}_1({}^4\text{G}) - {}_6\text{A}_1({}^6\text{S})$ transition in Mn^{2+} ions^{33,34}.

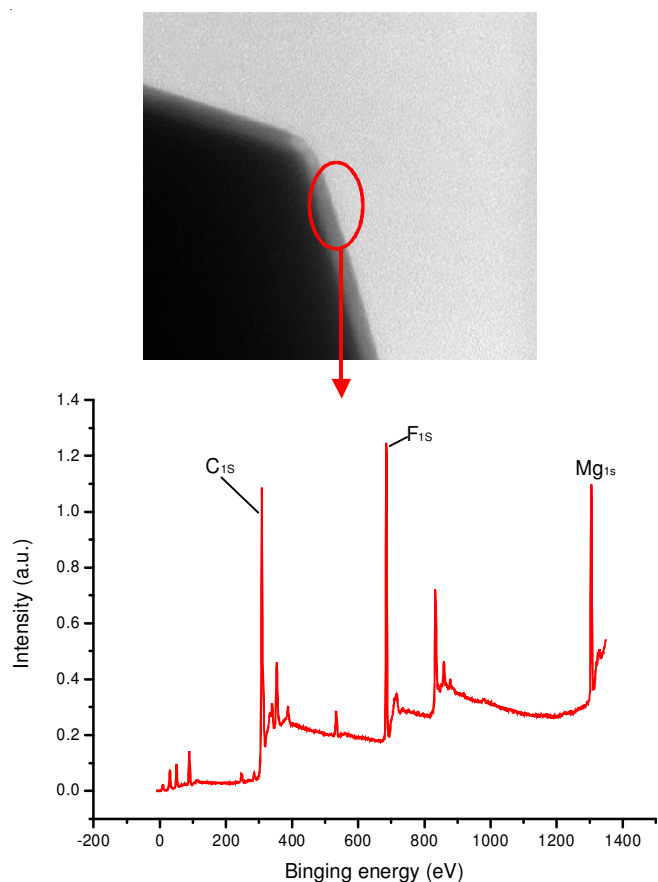


Fig. 3. XPS spectra of the coated layer on the surface of phosphor $\text{BaMgAl}_{10}\text{O}_{17}:\text{Eu}^{2+}, \text{Mn}^{2+}$

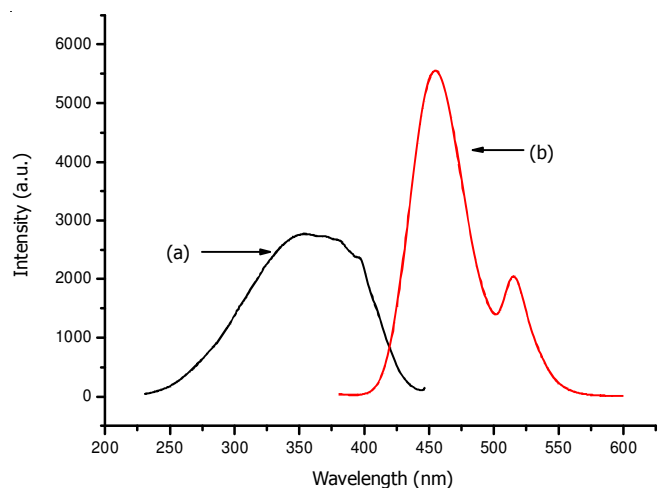


Fig. 4. Excitation ($\lambda_{\text{em}} = 450 \text{ nm}$) spectrum (a) and emission spectrum (b) of as-prepared $\text{BaMgAl}_{10}\text{O}_{17}:\text{Eu}^{2+}, \text{Mn}^{2+}$ phosphor

In order to clarify the energy transfer mechanism of $\text{BaMgAl}_{10}\text{O}_{17}:\text{Eu}^{2+}, \text{Mn}^{2+}$ phosphor, the Mn^{2+} doped concentration has increased from 0.05 mol % to 0.1 mol %. The luminescence intensities of samples with and without different Mn^{2+} doped concentration shown in Table-1. According to Dexter's energy transfer formula of multipolar interaction, the following relation can be obtained³⁵:

$$\frac{I_0}{I_m} = k \times C^{a/3} \quad \text{Formula (1)}$$

where, I_0 and I_m are the luminescence intensities of the sensitizer Eu^{2+} with and without activator Mn^{2+} present, K is a constant and C is then Mn^{2+} ion concentration. The plots of (I_0/I_m) versus $C^{\alpha/3}$ with $\alpha = 6, 8$ and 10 correspond to dipole-dipole, dipole-quadrupole and quadrupole-quadrupole interactions. When bring the figures in Table-1 to formula (1), the value of α is about 7.80, which close to 8. The result implies that the energy transfer from sensitizer Eu^{2+} to activator Mn^{2+} follows a non-radiative dipole-quadrupole mechanism, which is similar to the results of previous reports^{36,37}.

TABLE-1
LUMINESCENCE INTENSITIES OF $\text{BaMgAl}_{10}\text{O}_{17}:\text{Eu}^{2+}$
PHOSPHOR WITH DIFFERENT Mn^{2+} IONS DOPED
CONCENTRATION

Mn^{2+} ions doped concentration	0 mol %	0.05 mol %	0.1 mol %
Luminescence Intensity	7850	5800	956

The emission spectra of coated and uncoated phosphors are compared (Fig. 5). The relative emission intensity of uncoated phosphor decreased from 100 to 87 after thermal degradation tests, but those of samples coated with MgF_2 only decreases from 96.5 to 93.4, as compared to 100 for uncoated fresh phosphor. The decreased percentage of emission intensity of coated and uncoated samples is 13 % and 3.2 %, respectively. This indicates that the durability of BAM is greatly enhanced with the MgF_2 coating. The coated process keeps the oxygen out of the layer, so it could minimize the degradation of the phosphor³⁸. The degradation of BAM is due to conversion of Eu^{2+} to Eu^{3+} by oxygen, which can be suppressed by the coating.

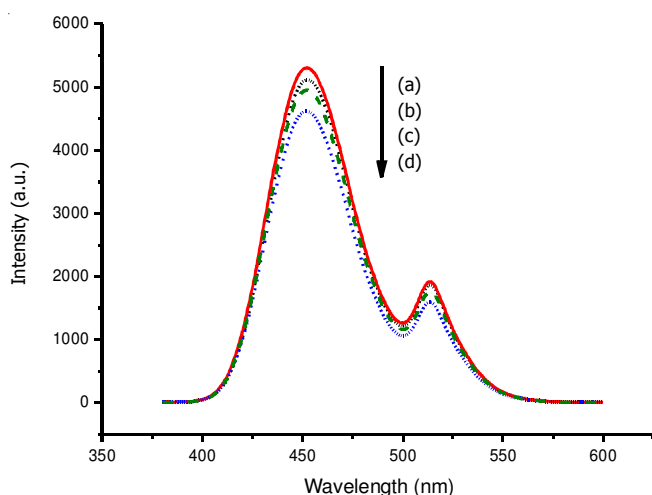


Fig. 5. Emission spectrum of phosphor samples in thermal test. (a) uncoated before thermal treatment; (b) coated before thermal treatment; (c) coated after thermal treatment; (d) uncoated after thermal treatment

Fig. 6 is the coordinates of the white LED by combining GaN chip (380 nm) with red-emitting phosphor $\text{Y}_2\text{O}_2\text{S}:\text{Eu}^{3+}$, green-emitting phosphor $\text{ZnS}:\text{Cu}^+, \text{Al}^{3+}$ and the blue-emitting phosphor $\text{BaMgAl}_{10}\text{O}_{17}:\text{Eu}^{2+}$, Fig. 6(a) is samples doped with Mn^{2+} and Fig. 6(b) is that of un-doped Mn^{2+} , under the same forward bias current in the CIE 1931 chromaticity diagram. The calculated colour coordinates of the samples white LED are located in that of standard illumination areas of (a) and

(b), which is close to that of the standard white light point of (0.333, 0.333). The right part of Fig. 6 showed the co-doped with Mn^{2+} samples has a more close colour coordinate to the standard white point and the colour rendering index increases from 79 to 85 after doped Mn^{2+} . It can be concluded that the tri-colour white LED is suitable for solid-state lighting application by improving the performance of the near UV LED phosphors.

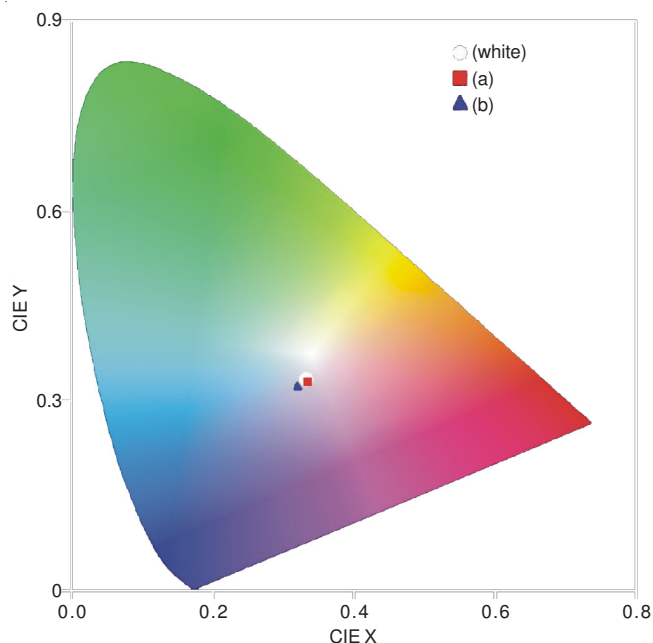


Fig. 6. Colour coordinates of the white LED combining GaN chip (380 nm) with tri-colour phosphor, which calculated using the software GoCIE. (a) with Mn^{2+} co-doping, (0.335, 0.330); (b) without Mn^{2+} doping, (0.320, 0.323); (white) standard white light point, (0.333, 0.333)

Conclusion

Phosphors $\text{BaMgAl}_{10}\text{O}_{17}:\text{Eu}^{2+}, \text{Mn}^{2+}$ were prepared by conventional solid-state reaction method and coated with MgF_2 by sol-gel route. XRD showed the doping and coating processes did not change the host crystal structure. SEM and TEM images exhibited that 25 nm to 30 nm thick layer was coated on the surface of the samples. Photoluminescence indicated that $\text{BaMgAl}_{10}\text{O}_{17}:\text{Eu}^{2+}, \text{Mn}^{2+}$ had a broad absorption band from near UV to blue and a second intense peak appeared at the 524 nm after doped Mn^{2+} . The mechanism of energy transfer between Eu^{2+} and Mn^{2+} was dipole-quadrupole. The durability of coated sample was greatly enhanced by the coating process. The Mn^{2+} doped samples had more close colour point to standard and high colour rendering index than the un-doped samples. All the result could conclude that co-doping and surface coating are two promising approaches for improve the colour rendering index of the near UV LED and the stability of $\text{BaMgAl}_{10}\text{O}_{17}:\text{Mn}^{2+}, \text{Eu}^{2+}$ phosphor.

ACKNOWLEDGEMENTS

This work supported by the National Natural Science Foundation of China (No. 51072234) and financially supported from the Hunan Steady New Material Company.

REFERENCES

1. Z.L. Wang, H.B. Liang, J. Wang, M.L. Gong and Q. Su, *Appl. Phys. Lett.*, **89**, 0719211 (2006).
2. X.S. Yan, W.W. Li and K. Sun, *J. Alloys Compd.*, **508**, 475 (2010).
3. R. Zhang and X. Wang, *J. Alloys Compd.*, **509**, 1197 (2011).
4. T.G. Kim, Y.S. Kim and S.J. Im, *J. Electrochem. Soc.*, **156**, 203 (2009).
5. P.L. Li, L.B. Pang, Z.J. Wang, Z.P. Yang, Q.L. Guo and X. Li, *J. Alloys Compd.*, **478**, 813 (2009).
6. S. Nakamura and G. Fasol, *The Blue Laser Diode: GaN Based Light Emitters and Lasers*; Springer Verlag: Berlin, (1997).
7. K.Y. Jung, H.W. Lee and H.K. Jung, *Chem. Mater.*, **18**, 2249 (2006).
8. Y.Q. Li, A.C.A. Delsing and H.T. Hintzen, *Chem. Mater.*, **17**, 3242 (2005).
9. Y.C. Liao, C.H. Lin and S.L. Wang, *J. Am. Chem. Soc.*, **127**, 9986 (2005).
10. Z. Zhou, F. Wang, S. Liu, K. Huang, Z. Li, S. Zeng and K. Jiang, *J. Electrochem. Soc.*, **158**, H1238 (2011).
11. C.W. Cho, C. Kim, W.I. Park, J.G. Yeo, K.J. Kim, Y.C. Kim, D.S. Zang and U. Paik, *Mater. Chem. Phys.*, **113**, 909 (2009).
12. P. Zhu and Q. Zhu, *Opt. Mater.*, **30**, 930 (2008).
13. S.H. Sohn and J.H. Lee, *J. Lumin.*, **129**, 478 (2009).
14. Y. Kim and S. Kang, *Appl. Phys. A.*, **98**, 245 (2009).
15. H. Zhu and H. Yang, *Mater. Lett.*, **62**, 784 (2008).
16. D.L. Deadmore, J.S. Machin and A.W. Allen, *J. Am. Ceram. Soc.*, **44**, 105 (1961).
17. T. Murata, H. Ishizawa, I. Motoyama and A. Tanaka, *J. Sol-Gel Sci. Technol.*, **32**, 161 (2004).
18. D.R. Messier, *J. Am. Ceram. Soc.*, **48**, 452 (1965).
19. S. Ruediger, U. Gross and E. Kemnitz, *J. Fluorine Chem.*, **128**, 353 (2007).
20. M. Wojciechowska, M. Zielinski and M. Pietrowski, *J. Fluorine Chem.*, **120**, 1 (2003).
21. M. Scrocco, *Phys. Rev. B.*, **33**, 7228 (1986).
22. Z. Zhou, F. Wang, S. Liu, K. Huang, Z. Li, S. Zeng and K. Jiang, *Asian J. Chem.*, **24**, 747 (2012).
23. T. Pilvi, T. Hatanpaa, E. Puukilainen, K. Arstila, M. Bischoff, U. Kaiser, N. Kaiser, M. Leskela and M. Ritala, *J. Mater. Chem.*, **17**, 5077 (2007).
24. S. Ali, N. Zahra, B. Sofiane and W.P. Monika, *J. Fluorine Chem.*, **131**, 1353 (2010).
25. W.J. Yang, L. Luo, T.M. Chen and N.S. Wang, *Chem. Mater.*, **17**, 3883 (2005).
26. J.S. Kim, K.T. Lim, Y.S. Jeong, P.E. Jeon, J.C. Choi and H.L. Park, *Solid State Commun.*, **21**, 135 (2005).
27. A.A. Setlur, J.J. Shiang and U. Happek, *Appl. Phys. Lett.*, **92**, 081104 (2008).
28. C. Guo, L. Luan, X. Ding, F. Zhang, F.G. Shi, F. Gao and L. Liang, *Appl. Phys. B: Laser Opt.*, **95**, 779 (2009).
29. C.Y. Shen, Y. Yang, S.Z. Jin and J.Z. Ming, *Physica B*, **405**, 1045 (2010).
30. C.H. Huang, W.R. Liu and T.M. Chen, *J. Phys. Chem. C*, **114**, 18701 (2010).
31. Y.R. Do, D.H. Park, H.G. Yang, W. Park, B.K. Wagner, K. Yasuda and C.J. Summers, *J. Electrochem. Soc.*, **148**, G548 (2001).
32. C.R. Ronda and B.M.J. Smets, *J. Electrochem. Soc.*, **136**, 570 (1989).
33. Y. Hao and Y. Wang, *J. Lumin.*, **122**, 1006 (2007).
34. R.P.S. Chakradhar, B.M. Nagabhushana, G.T. Chandrappa, K.P. Ramesh and J.L. Rao, *J. Chem. Phys.*, **121**, 10250 (2004).
35. D.L. Dexter and J.H. Schulman, *J. Chem. Phys.*, **22**, 1603 (1954).
36. W.J. Yang and T.M. Chen, *Appl. Phys. Lett.*, **88**, 101903 (2006).
37. W.R. Liu, Y.C. Chiu, Y.T. Yeh, S.M. Jang and T.M. Chen, *J. Electrochem. Soc.*, **156**, J165 (2008).
38. H. Yang, X.J. Wang, G.H. Duan, Y.M. Cui, L.C. Shen, Y.H. Xie and S.D. Han, *Mater. Lett.*, **58**, 2374 (2004).